

Numerical study of an internal-reforming solid oxide fuel cell and adsorption chiller co-generation system

Y. Liu, K.C. Leong*

School of Mechanical and Aerospace Engineering, Nanyang Technological University, 50 Nanyang Avenue, Singapore 639798, Singapore

Received 5 July 2005; accepted 27 October 2005

Available online 20 December 2005

Abstract

A study is conducted on a cogeneration system that incorporates a natural gas fed internal-reforming solid oxide fuel cell (IRSOFC) and a zeolite/water adsorption chiller (AC). The main aim is to investigate the performance of this combined system under different operating conditions and design parameters. A mathematical model is developed to simulate the combined system under steady-state conditions. The effects of fuel flow rate, fuel utilization factor, circulation ratio, mass of adsorbent and inlet air temperature on the performance are considered. The results show that the proposed IRSOFC-AC cogeneration system can achieve a total efficiency (combined electrical power and cooling power) of more than 77%. The electrical efficiency is found to decrease as the fuel flow rate increases, while the cooling power increases to a constant value. The total efficiency reaches a maximum value with variation of the fuel utilization factor. Both the circulation ratio and the inlet air temperature exert positive impacts on system efficiency.

© 2005 Elsevier B.V. All rights reserved.

Keywords: Solid oxide fuel cell; Adsorption cooling; Modelling; Cogeneration system; Internal reforming; Efficiency

1. Introduction

Solid oxide fuel cells (SOFCs) have been considered to be promising energy conversion technologies because they can provide a highly efficient rate of energy conversion with low pollutant emissions. The chemical energy of the fuel gas is converted directly to electricity in a SOFC, and hence it is expected that high electrical efficiencies can be achieved. The high operating temperature of SOFCs allows the use of cogeneration and hybrid systems. Gas–solid adsorption cooling systems are environmental-friendly compared with traditional CFC systems based on the vapour compression cycle as they employ safe and non-polluting refrigerants. Another advantage of adsorption cooling systems is that they can be driven by waste heat or solar energy. As a result, both SOFCs and adsorption cooling systems have attracted much research attention in the recent years.

Fuel cell cogeneration systems (FCCS) have been applied successfully in some developed countries. There have been

increased interests in such systems because they can achieve higher efficiency in electricity production and a higher overall efficiency with a low level of adverse environmental impact. One type of fuel cell and absorption cogeneration system has been investigated by several researchers [1,2] to produce electrical power and cooling simultaneously. Because the gas–solid adsorption cooling system is more flexible in operation compared with the absorption cooling cycle [3], a combined fuel cell and adsorption cooling cogeneration system can be a promising alternative.

In this paper, an internal-reforming solid oxide fuel cell (IRSOC) and a zeolite/water adsorption chiller (AC) cogeneration system is proposed. A numerical model based on the first law of thermodynamics is developed to simulate this combined system under steady-state operating conditions. The main aim is to investigate the performance of the combined system under different operating conditions and parameters.

2. System description

A schematic of the proposed SOFC and adsorption chiller cogeneration system is shown in Fig. 1. The system incorporates

* Corresponding author. Tel.: +65 6790 4725; fax: +65 6792 2619.
E-mail address: mkcleong@ntu.edu.sg (K.C. Leong).

Nomenclature

a	flow rate (kmol h^{-1})
E	cell voltage (V)
E_{re}	reversible cell voltage (V)
F	Faraday constant ($96,487 \text{ C mol}^{-1}$)
i	current density (mA cm^{-2})
i_0	exchange current density (mA cm^{-2})
I	current (A)
K_p	equilibrium constant
n	number of electrons participating in the reactions
p	pressure (bar)
Q	heat transfer rate (kJ h^{-1})
r_a	circulation ratio
R	universal gas constant ($8.314 \text{ J mol}^{-1} \text{ K}^{-1}$)
T	temperature (K)
U_f	fuel utilization factor

Greek letters

β	transfer coefficient
δ	thickness (cm)
ΔH	enthalpy of formation (kJ mol^{-1})
η_{act}	activation over-potential (V)
η_{conc}	concentration over-potential (V)
η_{ohmic}	ohmic over-potential (V)
η_t	total efficiency

Subscripts

a	anode
c	cathode
r	reforming reaction
s	shifting reaction

Superscripts

f	fuel
i	inlet
o	outlet

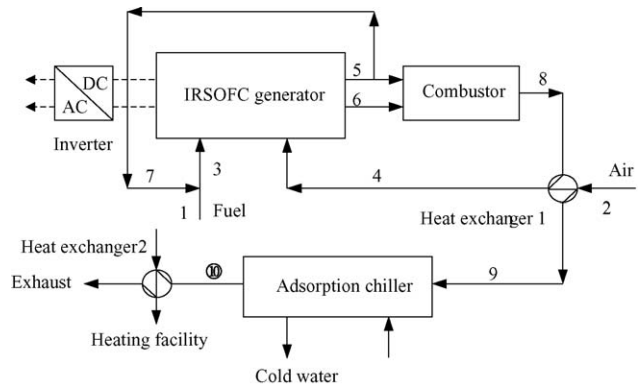


Fig. 1. Schematic of SOFC and adsorption chiller cogeneration system.

and its adsorption properties are also stable under high temperature. Finally, the gases from the adsorption chiller are passed through heat exchanger 2 for heat generation and then exhausted to the environment.

3. Numerical modelling

The numerical model consists of three parts: (i) internal reforming and electrochemical reaction model; (ii) SOFC model; (iii) adsorption cooling cycle model. The following assumptions are made: (i) equilibrium reforming and shifting reactions; (ii) the exit temperature of the cathode is equal to that of the anode; (iii) the SOFC and heat exchangers are in thermal balance; (iv) the burner efficiency is assumed to be 100%; (v) the mass of the adsorbent is proportional to the surface area of the adsorber; (vi) there is no heat loss in the cogeneration system.

3.1. Internal reforming and electrochemical reaction model

The recirculated anode exhaust fuel gas and the high-temperature conditions greatly assist the internal reforming and shifting reactions in a SOFC. The mechanisms for internal reforming and electrochemical reactions for the SOFC are commonly reported in the literature [4–7]. The reactions are:

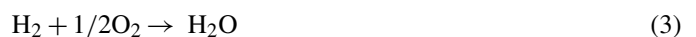
reforming reaction:



shifting reaction:



electrochemical reaction:



where the reforming and shifting reactions are assumed to reach thermodynamic equilibrium with the respective equilibrium constants represented by:

$$K_{p,r} = \frac{p_{\text{H}_2}^3 \cdot p_{\text{CO}}}{p_{\text{CH}_4} \cdot p_{\text{H}_2\text{O}}}; \quad K_{p,s} = \frac{p_{\text{CO}_2} \cdot p_{\text{H}_2}}{p_{\text{CO}} \cdot p_{\text{H}_2\text{O}}} \quad (4)$$

a natural gas feed, an IRSOFC, an AC, a dc–ac inverter, and two heat exchangers. The system can produce electricity, cooling and heating simultaneously. Air is preheated at the heat exchanger before it enters the IRSOFC generator. Part of the exhaust fuel gas is recirculated and mixed with fresh fuel gas and the mixture re-enters the IRSOFC. Fuel gas and air flow through the anode and cathode, respectively. Fuel gas is internally reformed at the anode and hydrogen is produced. The electrochemical reaction occurs in the SOFC and electricity is generated together with heat. Subsequently, the non-recirculated portion of the effluent fuel gas and depleted air flow into a combustor. After reacting in the combustor, the fuel–air mixture enters heat exchanger 1 where the air is preheated. The combustion gases exiting from heat exchanger 1 then flows through the adsorption chiller to drive this cooling system during the heating process. Zeolite/water is used as the working pair for the adsorption chiller. Zeolite has satisfactory adsorption ability

The equilibrium constants are considered to be functions of temperature and can be obtained from the following equation:

$$\log K_p = AT^4 + BT^3 + CT^2 + DT + E \quad (5)$$

The values of the parameters in Eq. (5) have been reported in literature [8]. It is assumed that the fresh fuel gas is composed of CH₄, N₂ and CO₂. The equilibrium constants can be rewritten as:

$$K_{p,r} = \frac{\left(\frac{x-y}{a_1^f+2x}\right) \left(\frac{3x+y-z}{a_1^f+2x}\right)^3 p_{\text{cell}}^2}{\left(\frac{a_{\text{CH}_4}^f-x}{a_1^f+2x}\right) \left(\frac{z-x-y}{a_1^f+2x}\right)} \quad (6)$$

$$K_{p,s} = \frac{\left(\frac{3x+y-z}{a_1^f+2x}\right) \left(\frac{a_{\text{CO}_2}^f+y}{a_1^f+2x}\right) p_{\text{cell}}^2}{\left(\frac{x-y}{a_1^f+2x}\right) \left(\frac{z-x-y}{a_1^f+2x}\right)} \quad (7)$$

where x , y and z are the reactant molar flow rates of CH₄, CO₂ and H₂, respectively, and the superscript f denotes fresh fuel gas.

The reactant flow rate z of hydrogen can be obtained from the fuel utilization factor as follows:

$$z = U_f(4a_{\text{CH}_4}^i + a_{\text{H}_2}^i + a_{\text{CO}}^i) \quad (8)$$

where the superscript i represents inlet cell and U_f is the fuel utilization factor.

If the value of the circulation ratio r_a is known, Eq. (8) can be rewritten as:

$$z = \frac{4U_f \cdot a_{\text{CH}_4}^f}{1 - r_a + r_a \cdot U_f} \quad (9)$$

3.2. SOFC model

The cell voltage calculation is the core of the SOFC model. The cell electrical power can be calculated as the product of the cell current and the cell voltage, while the cell current can be easily obtained from a known value of the fuel utilization factor. Based on the work of several researchers [6,9,10], the cell voltage is given by:

$$E = E_{\text{re}} - (\eta_{\text{act}} + \eta_{\text{ohm}} + \eta_{\text{conc}}) \quad (10)$$

where E_{re} is the ideal reversible cell voltage and the other three terms represent the activation, ohmic and concentration overpotentials.

The ideal reversible cell voltage can be evaluated from the Nernst equation, i.e.

$$\begin{aligned} E_{\text{re}} &= E_0 - \frac{RT}{2F} \ln \left(\frac{p_{\text{H}_2\text{O}}}{p_{\text{H}_2} p_{\text{O}_2}^{1/2}} \right) \\ &= \frac{RT \ln K_{p,e}}{2F} - \frac{RT}{2F} \ln \left(\frac{p_{\text{H}_2\text{O}}}{p_{\text{H}_2} p_{\text{O}_2}^{1/2}} \right) \end{aligned} \quad (11)$$

where $K_{p,e}$ is the equilibrium constant of the electrochemical reaction.

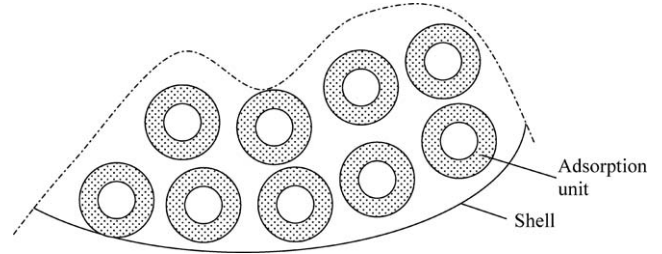


Fig. 2. Schematic of adsorber in adsorption chiller.

The anode and cathode activation overpotentials can be described by the Butler–Volmer equation [11]:

$$i = i_0 \left[\exp \left((1 - \beta) \frac{F\eta_{\text{act}}}{RT} \right) - \exp \left(-\beta \frac{F\eta_{\text{act}}}{RT} \right) \right] \quad (12)$$

where β is the transfer coefficient and i_0 is the apparent exchange-current density.

The ohmic overpotential as suggested by Bessette [11] is given by

$$\eta_{\text{ohmic}} = i \sum_j \rho_j \delta_j = i \sum_j A_j \exp \left(\frac{B_j}{T} \right) \delta_j \quad (13)$$

The parameters A_j and B_j are constants for different components, while δ_j is the thickness of the cell components.

The concentration overpotential is a result of the reactant diffusion during reaction. According to Bove et al. [10], concentration losses can be ignored under normal operating conditions. The SOFC current can be quantified using the fuel utilization factor, U_f , i.e.,

$$I = znF = 2FU_f(4a_{\text{CH}_4}^i + a_{\text{H}_2}^i + a_{\text{CO}}^i) \quad (14)$$

The SOFC only converts part of the chemical energy of the fuel into electrical power while the remainder will become heat to increase the temperature of the outlet effluent gas. From the following energy-balance equation, the temperature of outlet gas is computed.

$$\begin{aligned} \sum_j a_{j,c}^i \Delta H_{j,c}^i + \sum_j a_{j,a}^o \Delta H_{j,a}^i \\ = \sum_j a_{j,c}^o \Delta H_{j,c}^o + \sum_j a_{j,a}^o \Delta H_{j,a}^o + EI \end{aligned} \quad (15)$$

As the temperature is known from Eq. (15) and for a specified fuel utilization factor and inlet conditions, the species concentration in the SOFC can be obtained by solving Eqs. (6)–(8).

3.3. Adsorption cooling cycle model

After preheating the air, the gas from combustor is directed to the zeolite/water adsorption chiller. The adsorber consists of a number of adsorption units, as shown schematically in Fig. 2. Every adsorption unit is a metal tube covered with a zeolite adsorbent bed. The configuration is the same as that of the adsorber described in our previous paper [12]. The exhaust gas from heat exchanger 1 flows through the metal tube of the adsorption

unit and heats up the zeolite adsorbent bed. The heat and mass balance equations for every adsorption unit here are the same as those reported previously [12] except that the heat-exchange fluid is changed to the exhaust gas. Adsorption chillers with a continuous adsorption cycle are employed in this system. Hence, the cooling power can be presented as:

$$P_{\text{cw}} = \frac{N \cdot m_s \Delta q [L(T_e) - C_{\text{pl}}(T_c - T_e)]}{t_h} \quad (16)$$

where N is the number of adsorption units; m_s is the mass of the adsorbent for every adsorption unit; t_h is the duration of the heating process; Δq is the change of adsorbed water uptake.

3.4. Modelling of combustor and other components

It is assumed that the exhaust gas from the SOFC is completely burnt in the combustors, i.e., CO and H₂ in the exhaust gas are converted to CO₂ and H₂O, respectively. Thus, the heat-balance equation of the combustor is:

$$\sum_j a_j^i \Delta H_j^i = \sum_j a_j^o \Delta H_j^o \quad (17)$$

The heat-balance equation for the heat exchangers is similar to the above equation with no species change in the heat exchangers.

4. Calculations for system model

A flow chart of the modelling calculations for the SOFC-AC system is presented in Fig. 3. The results of every block in the flow chart become the inputs for the next block. After setting the process parameters, the calculation block belonging to the SOFC model will be executed several times until the error of the energy balance is less than the assigned tolerance (0.1 K). Other blocks in Fig. 3 will only be executed once. In this study, the SOFC is assumed to be in thermal equilibrium with the exhaust gas. Thus, by making an initial guess of the cell temperature, the equilibrium data for the three reactions in the SOFC can be obtained. All characteristics of the exhaust gas from the anode and cathode can be obtained by solving Eqs. (6)–(9). Using this data, the SOFC performance can be obtained in terms of cell voltage and cell current. The energy-balance equation can be used to assess the validity of the guessed temperature. When the cell temperature is confirmed and the characteristics of the exhaust gas from the SOFC are calculated, the subsequent calculation blocks will be solved one by one. The output data of the former block is the input of the next block. The numerical method for the calculation of adsorption cycle block has been described previously [12]. Visual FORTRAN software was used to develop the simulation code for this SOFC-AC model.

5. Results and discussion

The results of the numerical model can be used to carry out a detailed parametric analysis which can provide an insight into the effects of variation of the operating parameters on the per-

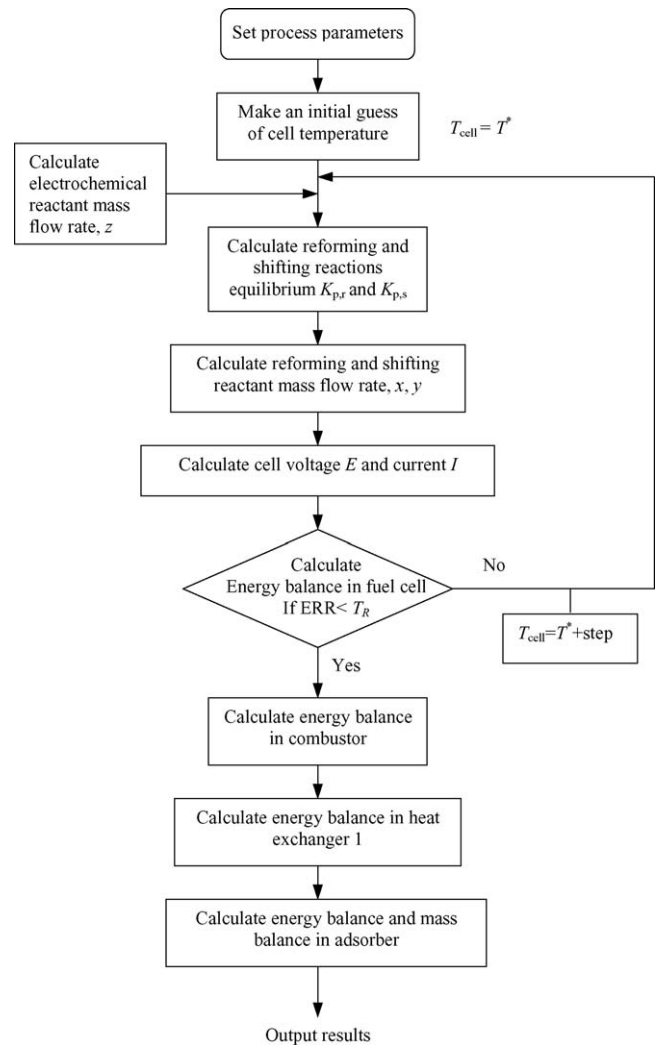


Fig. 3. Flow chart of calculations for SOFC-AC system.

formance of SOFC systems. The operating parameters for the base case are shown in Table 1. In this study, heat power is not considered. Thus, the total efficiency of SOFC-AC system is given by:

$$\eta_t = \frac{P_{\text{ew}} + P_{\text{cw}}}{\text{LHV}} \quad (18)$$

where P_{ew} is the electrical power delivered by the SOFC and LHV is the lower heating value of the inlet fuel. Simulated results for the base case show that the SOFC operates at a voltage of 0.775 V and a current density of 150 mA cm⁻². The SOFC-AC cogeneration system can achieve a total efficiency of more than 77%, i.e. electrical power 62% and cooling power 15%. About 1800 kW of electrical power and 450 kW of cooling power can be produced by the system. The simulated stream properties for the base case are shown in Table 2.

5.1. Effect of inlet fuel flow-rate

The effect of inlet fuel flow-rate on system efficiency is presented in Fig. 4. Here the ratio of the inlet fuel flow-rate to the

Table 1
Prescribed values of parameters for base case

Parameters	Value
Fuel inlet composition	CH ₄ : 84%, N ₂ : 15%, CO ₂ : 1%
Fuel inlet temperature	300 K
Air inlet temperature	300 K
Air temperature after preheat	930 K
Cell operating pressure	1.0 bar
dc/ac inverter efficiency	95%
Burner efficiency	100%
Fuel utilization factor, U_f	0.8
Circulation ratio, r_a	0.2
Electrolyte thickness	0.015 cm
Interconnect thickness	0.010 cm
Cathode thickness	0.20 cm
Anode thickness	0.020 cm
Half cycle time of adsorbent cycle, t_h	1200 s
Mass of the adsorbent, m_s	5 kg
Number of adsorption units, N	250

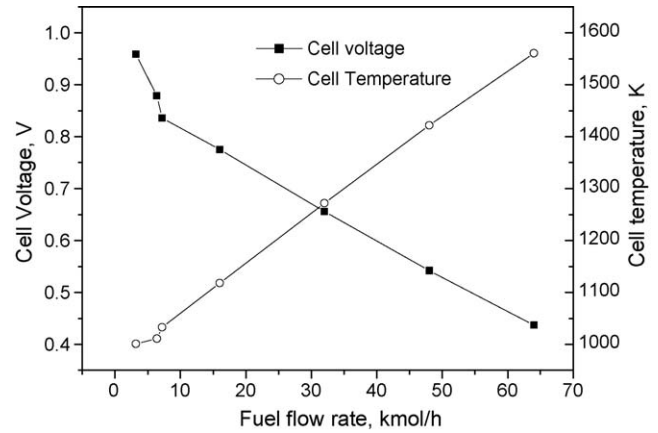


Fig. 5. Effect of fuel flow-rate on cell voltage and cell temperature.

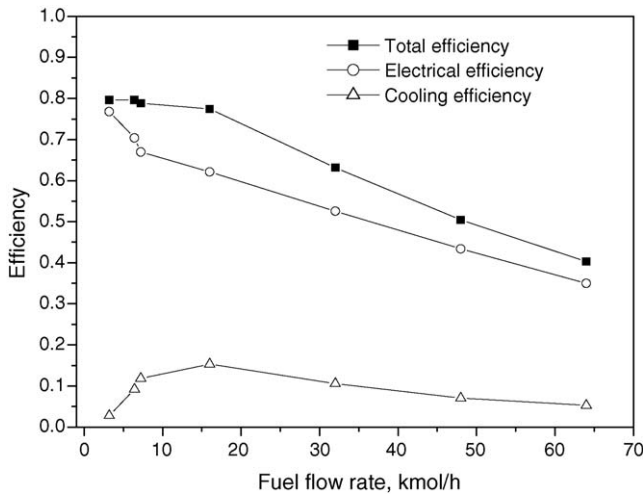


Fig. 4. Effect of fuel flow-rate on efficiency.

inlet air fuel-flow rate is fixed. The data show that both the electrical efficiency and total efficiency decrease as the fuel flow-rate increases, while the cooling efficiency has a maximum value for the range of fuel flow-rates investigated. The effect of fuel

flow-rate on cell voltage and cell temperature is presented in Fig. 5. For a constant fuel utilization factor and circulation ratio, a higher rate of fuel flow means that more current will be produced and hence, the current density is increased. The higher the current density, the higher is the value of the total overpotential produced. The increase in overpotential will result in a reduction in the voltage of SOFC (see Fig. 5). Since current has a linear relationship with fuel flow-rate, the electrical efficiency will decrease. It is shown in Fig. 5 that the cell temperature increases linearly with an increase in the inlet flow-rate. The increase in overpotential will increase heat generation, which will raise the cell temperature. The effect of inlet fuel flow-rate on cooling power is shown in Fig. 6. The cooling power increases asymptotically to a constant value with increase in the fuel flow-rate. When the fuel flow-rate increases, the electrical efficiency will decrease. This means that more heat can be generated in the combustor. Thus, the driven temperature of the adsorption chiller also increases and this leads to an increase in cooling power for a fixed cycle time. When the driven temperature increases to a certain value, no more refrigerant can be drawn from the adsorbent. Thus, the value of the cooling power will tend to a constant value and the cooling efficiency will decrease.

Table 2
Stream properties for SOFC-AC system

	Temperature (K)	Gas flow rate (kmol h ⁻¹)	Gas composition (%)						
			CH ₄	H ₂	CO	CO ₂	H ₂ O	N ₂	O ₂
1	300	16	84.0	–	–	1.0	–	15.0	–
2	300	180	–	–	–	–	–	79	21
3	608	26.7	50.3	5.5	2.9	10.4	19.7	11.2	–
4	930	180	–	–	–	–	–	79	21
5	1118	53.6	–	13.6	7.2	24.5	49	5.7	–
6	1118	157.6	–	–	–	–	–	90.2	9.8
7	1118	10.7	–	13.6	7.2	24.5	49	5.7	–
8	1481	196	–	–	–	6.9	13.7	73.8	5.6
9	934	196	–	–	–	6.9	13.7	73.8	5.6
10	^a	196	–	–	–	6.9	13.7	73.8	5.6

^a Temperature of stream 10 will change with time.

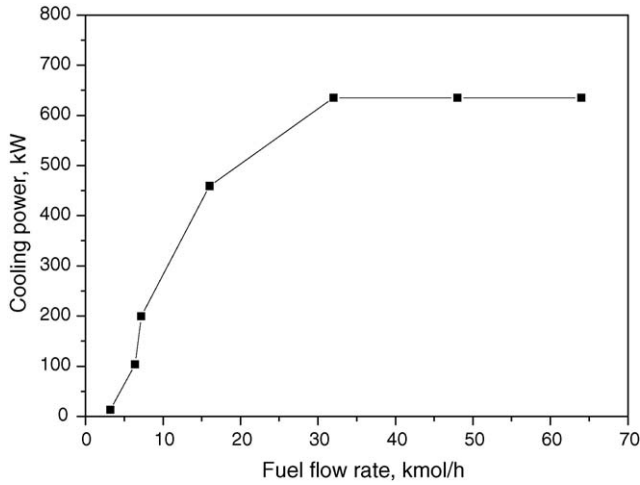


Fig. 6. Effect of fuel flow-rate on cooling power produced.

5.2. Effect of fuel utilization factor

The effect of the fuel utilization factor U_f , on system performance is shown in Fig. 7, while the effect on cell voltage and cell temperature is given in Fig. 8. When the fuel utilization factor increases, the content of hydrogen in the anode is reduced. A higher U_f will lead to a higher value of current and a higher cell temperature (see Fig. 8). The cell temperature reduces the overpotential and the current gives rise to an increased overpotential. The SOFC voltage will increase slightly and then decrease quickly with increase U_f due to the combined effect of cell temperature and current density. The electrical efficiency, which is proportional to the product of voltage and U_f , has a maximum value at a U_f around 0.85. For a U_f value larger than 0.85, the electrical efficiency will decrease due to the increased effects of the voltage drop. A higher U_f also results in a lower combustion temperature, that leads to a lower value of the driven temperature for the adsorption chiller. Therefore, the cooling power will decrease with higher U_f . When U_f increases beyond

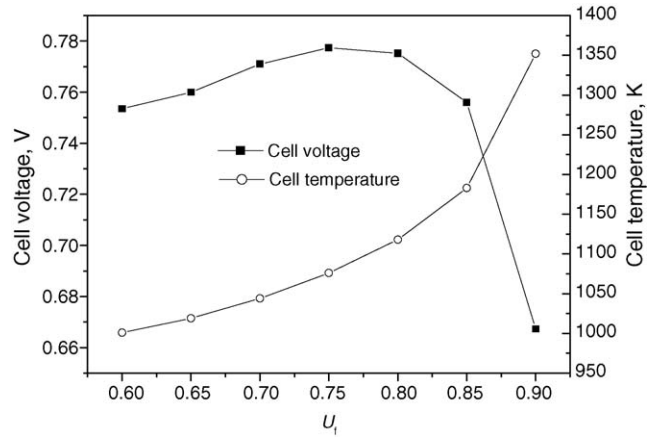


Fig. 8. Effect of fuel utilization factor on cell voltage and cell temperature.

0.85, the electrical efficiency will decrease, which in turn leads to a higher depleted fuel heating value. Thus, more heat will be generated in the combustor and the driven temperature of adsorption chiller will increase. Therefore, the cooling power and the cooling efficiency will increase with increase in fuel utilization factor when $U_f > 0.85$.

5.3. Effect of circulation ratio

The effect of circulation ratio on system performance is shown in Fig. 9. It can be seen that an increase in the circulation ratio has a positive impact on the system electrical efficiency, but adversely affects the cooling efficiency. The total efficiency can increase slightly with an increase in the circulation ratio. If the circulation ratio increases, the global fuel utilization factor will also increase. Hence, the electrical efficiency increases for a higher value of the circulation ratio. A high circulation ratio also leads to a lower depleted fuel heating value, and hence, a lower driven temperature in the adsorption chiller. The latter leads to a decrease in cooling power for a fixed cycle time. Hence, for fixed inlet fuel flow-rate, the cooling efficiency will decrease

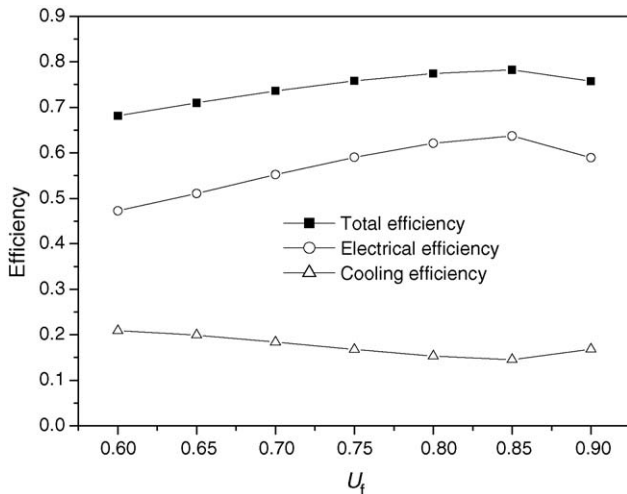


Fig. 7. Effect of fuel utilization factor on efficiency.

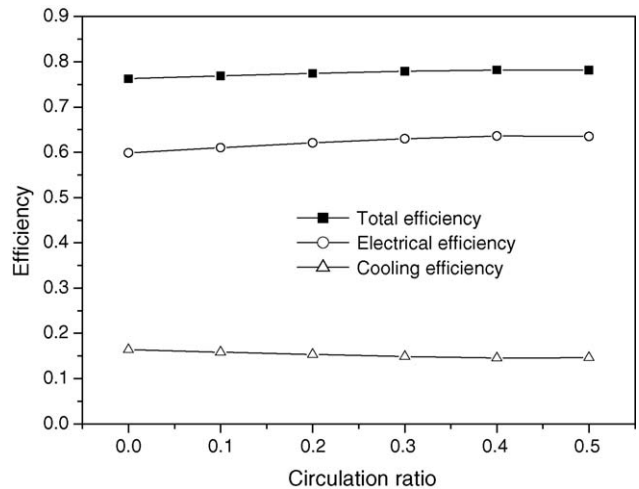


Fig. 9. Effect of circulation ratio on efficiency.

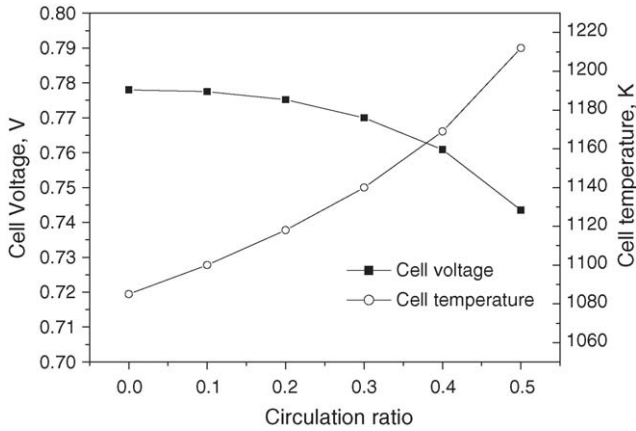


Fig. 10. Effect of circulation ratio on cell voltage and cell temperature.

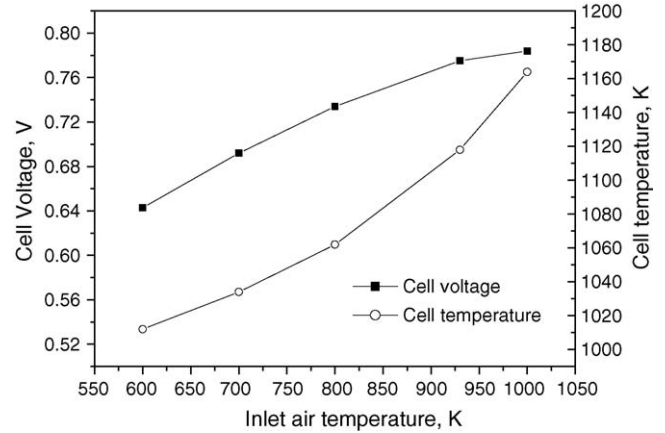


Fig. 12. Effect of inlet air temperature on cell voltage and cell temperature.

with increase in the circulation ratio. The effect of circulation ratio on cell voltage and cell temperature is given in Fig. 10. The trends of the curves are very similar to those in Fig. 8 as an increase of circulation ratio leads to a larger global utilization factor. Thus, effects on cell voltage and cell temperature for these two operating parameters are similar.

5.4. Effect of inlet air preheat temperature

The inlet air temperature can be increased by increasing the heat-exchange efficiency between air and the mixed gas from the combustor in heat exchanger 1. The influence of inlet air temperature on system efficiency is given in Fig. 11. An increase in the inlet air temperature yields an increase in the electrical efficiency and total efficiency which have a negative effect on cooling efficiency. A high value of the inlet air temperature will result in a high cell temperature and therefore result in an increase in the voltage (see Fig. 12). A high inlet air temperature also leads to a reduction in the temperature of the steam, which drives the adsorbent. Thus, the cooling power will be reduced with increase in the inlet air temperature.

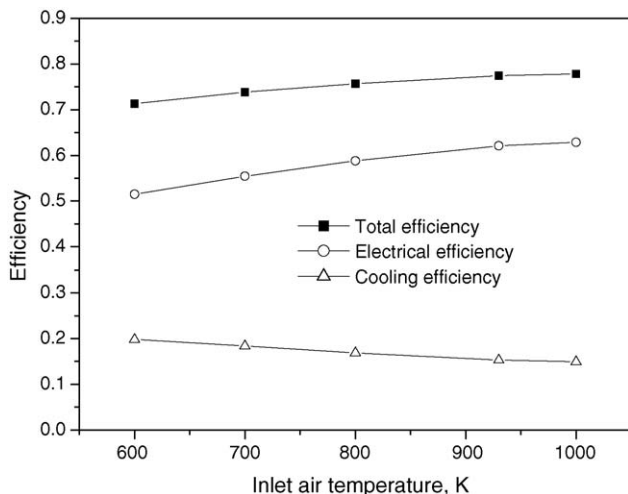


Fig. 11. Effect of inlet air temperature on efficiency.

5.5. Effect of mass of adsorbent

The effect of the mass of adsorbent on cooling power is presented in Fig. 13. The mass of zeolite adsorbent in the adsorbent is proportional to the number of adsorption units. Therefore, an increased mass of zeolite will lead to a reduction of the inlet mass flow of the exhaust gas from heat exchanger 1 for every adsorption unit. It was concluded in a previous study [13] that the thermal performance of the adsorption cycle will change very little when the mass flow-rate of the heat-exchange fluid is larger than a certain value. Hence, when the total mass of adsorbent increases, the cycled refrigerant produced by every adsorption unit changes negligibly. Thus, the total cycled refrigerant is increased for a larger mass of adsorbent, which leads to a higher value of cooling power. With a further increase in the mass of the adsorbent, the maximum temperatures of adsorbent decreases rapidly and causes a significant reduction in the cycled mass. Accordingly, the total cycled refrigerant begins to decrease. In summary, the cooling power has a maximum value with variation of the mass of adsorbent.

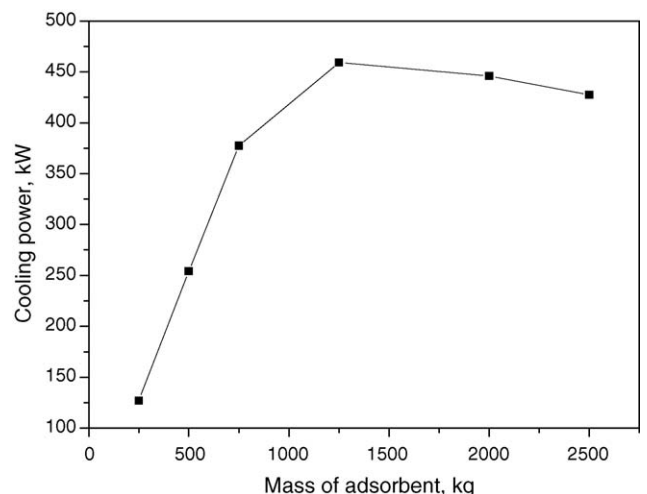


Fig. 13. Effect of mass of adsorbent on cooling power produced.

6. Conclusions

The effects of fuel flow-rate, circulation ratio, fuel utilization factor, inlet air temperature and mass of adsorbent on the performance of a IRSOC-absorption chiller system are investigated. Based on simulation results, the following conclusions can be drawn.

- (1) The proposed IRSOFC-adsorption chiller cogeneration system can achieve a total efficiency of more than 77% (electrical power of 62% and cooling power of 15%).
- (2) Both the electrical efficiency and total efficiency decrease as the fuel flow-rate increases. In addition, the cooling power increases asymptotically to a constant value with increase in the fuel flow-rate.
- (3) The electrical efficiency has a maximum value at a value of U_f of 0.85 within the investigated range.
- (4) An increase in the circulation ratio has a positive impact on the system electrical efficiency but adversely affects the cooling power.
- (5) An increase in the inlet air temperature yields an increase in both the electrical efficiency and the total efficiency. The

cooling power exhibits a maximum value with variation of the mass of adsorbent in the adsorption chiller.

References

- [1] J.L. Silveria, E.M. Leal, L. Ragonha Jr., *Energy* 26 (2001) 891–904.
- [2] M. Burer, K. Tanaka, D. Favrat, K. Yamada, *Energy* 28 (2003) 497–518.
- [3] N. Douss, F. Meunier, *Chem. Eng. Sci.* 44 (1989) 225–235.
- [4] A.F. Massardo, F. Lubelli, *J. Eng. Gas Turbines Power* 122 (2000) 27–35.
- [5] S. Campanari, *J. Power Sources* 92 (2001) 26–34.
- [6] S.H. Chan, H.K. Ho, Y. Tian, *J. Power Sources* 109 (2002) 111–120.
- [7] W. Zhang, E. Croiset, P.L. Douglas, M.W. Fowler, E. Entchev, *Energy Conv. Manage.* 46 (2005) 181–196.
- [8] U.G. Bossel, *Final Report on SOFC Data Facts and Figures*, Swiss Federal Office of Energy, Berne, CH, 1992.
- [9] D.J. Hall, *Transient modeling and simulation of a solid oxide fuel cell*, PhD Thesis, University of Pittsburgh, 1997.
- [10] R. Bove, P. Lunghi, N.M. Sammes, *Int. J. Hydrogen Energy* 30 (2005) 181–187.
- [11] N.F. Bessette, *Modeling and simulation of a solid oxide fuel cell power system*, PhD Thesis, Georgia Institute of Technology, 1994.
- [12] K.C. Leong, Y. Liu, *Appl. Therm. Eng.* 24 (2004) 2359–2374.
- [13] Y. Liu, K.C. Leong, *Appl. Therm. Eng.* 25 (2005) 1403–1418.